Sensors & Diagnostics

PAPER

View Article Online
View Journal | View Issue

Cite this: *Sens. Diagn.*, 2026, **5**, 404

Development of an integrated label-free electrochemical sensor with sample collection for the detection of *Acinetobacter baumannii*

Sallam Al-Madhagi,[a] Souna Elwary,[a] Luay Fawzi Abuqatouseh[b] and Mohammed Zourob *[a]

Acinetobacter, a genus of bacteria capable of infecting humans, is found in the healthcare environment. *Acinetobacter baumannii* (*A. baumannii*), which is one of the most important species in the genus *Acinetobacter*, causes bloodstream, wound, and pneumonia infections in immunocompromised patients. This bacterium adapts to various conditions and develops antibiotic resistance, making it challenging to manage in healthcare settings. In this study, an integrated label-free electrochemical sensor was developed for the detection of *A. baumannii* non-coding RNA (ncRNA). This integrated sensing platform, consisting of two parts: the sample collection unit and the detection electrode, has been developed. The sample collection was fabricated from paper for collecting the sample and integrated with a heating probe for lysing the bacteria and releasing the ncRNA. The detection mechanism relies on the hybridization of the bacterial ncRNA to the thiolated complementary sequences immobilized on the sensor surface. The sensor employed a three-electrode chip and square wave voltammetry (SWV). The increase in the current due to the hybridization event with the target ncRNA was quantified. To create a user-friendly sensor, sample collection pads were integrated with the electrochemical sensor, which was subsequently employed to collect and identify bacteria from contaminated surfaces. The developed sensor exhibits high selectivity and sensitivity, with a 5 pM limit of detection (LoD) and 15 pM limit of quantification (LoQ), respectively. It has been demonstrated that the sensor has the capability to detect non-coding RNA from *A. baumannii* in samples from cell cultures. This sensor offers a promising approach for direct bacterial detection in a single device, eliminating the need for multiple pre-test steps or DNA amplification.

Received 17th July 2025,
Accepted 1st December 2025

DOI: 10.1039/d5sd00130g

rsc.li/sensors

1. Introduction

Acinetobacter, a bacterial genus capable of infecting humans, is commonly found in aquatic and terrestrial environments.[1,2] It is also present in healthcare environments.[3,4] The resistance of these bacteria to numerous antibiotics renders the treatment of these infections particularly challenging. *Acinetobacter baumannii* (*A. baumannii*), the most significant species in the genus *Acinetobacter*, is responsible for infections in the bloodstream, wounds, and pneumonia in immunocompromised patients. This pathogen is challenging to manage in healthcare settings due to its ability to adapt to various environments and develop resistance to numerous antibiotics.[1,5–7]

The prolonged survival of *A. baumannii* in healthcare environments, attributed to its biofilm formation and desiccation resistance, increases the risk of transmission to susceptible patients.[8–10] Studying *Acinetobacter* in the medical field is crucial for comprehending its pathogenicity, developing effective treatment strategies, and instituting infection control measures to avert outbreaks in healthcare environments. Researchers can enhance patient outcomes and mitigate the global burden of healthcare-associated infections by comprehending the mechanisms of *A. baumannii* infection and early detection.[11–13]

Acinetobacter baumannii samples are often collected from contaminated surfaces using sterile swabs or compact sample-collecting pads.[14–16] *Acinetobacter baumannii* may be cultured or lysed for molecular detection.[1] Lysis is achieved by chemical or thermal disruption of the bacterial cell wall and membrane.[17,18] The resulting lysate, containing the desired sequence or protein, is then immediately used for detection testing. This sample adds a burden to the analysis protocol due to the need for several initial steps before the final test for this bacterium, which may be inaccessible in areas with inadequate infrastructure or regions far from central labs.

[a] *Department of Chemistry, Alfaisal University, Al Zahrawi Street, Al Maather, Al Takhassusi Road, Riyadh 11533, Saudi Arabia. E-mail: mzourob@alfaisal.edu*
[b] *Faculty of Pharmacy and Medical Sciences, Petra University, Jordan*

The diagnosis of *A. baumannii* is typically achieved using molecular testing, which is based on clinical laboratory results, in addition to bacteriological isolation and clinical specimen culturing.[19,20] However, identifying *A. baumannii* can be complex and requires specialized laboratories and trained personnel. Consequently, rapid testing utilizing portable tools that can be employed at the testing site could enhance efforts to mitigate these infections. To address the limitations of current methods, a sensitive, selective, and cost-effective tool is vital for detecting low levels of *A. baumannii.*[20]

Khalil *et al.*[21] and Bahavarnia *et al.*[22] reported methods for the detection of *A. baumannii* from other Gram-negative bacteria employing amplification and detection of DNA using colorimetric assay. Kanapathy *et al.*[23] reported electrochemical DNA-based detection, but it needs preliminary treatment, including DNA isolation and amplification, prior to the detection step. A limited number of sensors have been reported for the detection of entire bacteria, either through the modification of electrodes with molecularly imprinted polymers[24] or by employing aptamers as recognition components.[25]

Non-coding RNA (ncRNA) refers to RNA molecules that do not encode proteins, in contrast to messenger RNA (mRNA) and transfer RNA (tRNA).[26,27] In *Acinetobacter baumannii*, non-coding RNAs (ncRNAs) play an essential role in regulating gene expression, stress adaptability, and virulence.[28,29] Non-coding RNAs of *Acinetobacter baumannii* constitute a complex regulatory network that enhances survival, virulence, and antibiotic resistance under various environmental conditions.[30,31] The detection of ncRNA has several advantages, including a more precise, functional, and real-time representation of microbial activity and gene regulation in comparison with DNA amplification, rendering it especially beneficial for diagnostics, antimicrobial resistance research, and biosensor innovation.[32]

In this work, we have developed and optimized an integrated electrochemical sensor for the detection of *A. baumannii* ncRNA. The sensor is comprised of a paper sampling collection pad and heating lysing probe to lyse and release the ncRNA. Subsequently, the ncRNA was detected upon hybridization with immobilized complementary sequences on the electrode surface. This would facilitate bacterial detection at the infection site without necessitating pre-detection treatments.

2. Materials and methods

2.1. Materials

Thiolated single-strand oligonucleotides (capture probe), along with the complementary ncRNA sequences, for *Acinetobacter baumannii*, *Salmonella* ncRNA, and *Pseudomonas* ncRNA were synthesized by Metabion international AG (Planegg, Germany). The *Acinetobacter baumannii* ncRNA sequence was chosen for its high specificity to *Acinetobacter baumannii* after a thorough *in silico* analysis using the RNA database (https://rnacentral.org). BLAST was used to confirm its strong specificity. DEP-chip gold electrodes (ER-P series) were obtained from BioDevice Technology, Ltd. (Ishikawa, Japan). Each electrode consists of three integrated electrodes, including a gold working electrode (WE), a platinum counter electrode (CE), and a silver/silver chloride (Ag/AgCl) reference electrode (RE) patterned on a polyimide substrate.

Phosphate-buffered saline (PBS) (tablets) and bovine serum albumin (BSA) were obtained from Sigma-Aldrich S.A. (St. Louis, MO, United States).

2.2. Instrumentation and procedure

In order to carry out the electrochemical tests at room temperature in the traditional three-electrode configuration, an Autolab PGSTAT128N, a computer-controlled apparatus manufactured by Metrohm (Netherlands), was used. In all the electrochemical tests, a detection solution was used. This solution consisted of 10 mM PBS with a pH of 7.4 and 10 mM $[Fe(CN)_6]^{3-/4-}$. Every experiment was carried out with the assistance of NOVA software (version 1.11, used by Metrohm). Square wave voltammetry (SWV) measurements were performed using a voltage range extending from −0.2 to 0.6 V with a scan rate of 100 mV s^{-1}, a frequency of 25 Hz, an interval time of 0.04 s, a step potential of −5 mV, and an amplitude of 20 mV.

2.3. Cell culture and lysis

The bacteria of interest, *Acinetobacter baumanni* (ATCC 19606), was grown in a nutrient broth for 24 hours at 37 °C. Briefly, nutrient broth (peptone 5 g L^{-1}, beef extract 3 g L^{-1}, sodium chloride 5 g L^{-1}, pH 7.4) was prepared in distilled water, and the broth was sterilized by autoclaving at 121 °C for 15 min. *Acinetobacter baumannii* ATCC 19606 was revived from a −80 °C glycerol stock by streaking onto a blood agar plate using a sterile inoculating loop. The plate was incubated aerobically at 37 °C for 24 hours. A single colony was then inoculated into 5 mL nutrient broth and incubated at 37 °C for 24 h with shaking. The resulting culture was used for subsequent experiments.

For initial testing, the cultivated bacteria were lysed using a JY88-IINs ultrasonic homogenizer using 25 kHz at 30 percent power for one minute. The lysed bacterial suspension was passed through a 0.2 μm syringe to extract the RNA sequences. The fluid was gently pushed through the membrane into a clean collection tube. The resulting filtered fluid was used directly for sensor testing.

2.4. Sample collection and lysis

The sensing platform consists of two sites, as shown in Scheme 1. A laser writer was used to fabricate the required design in double-sided adhesive foil featuring two sites: a paper pad for sample collection, equipped with lateral flow sample pads, and the other for

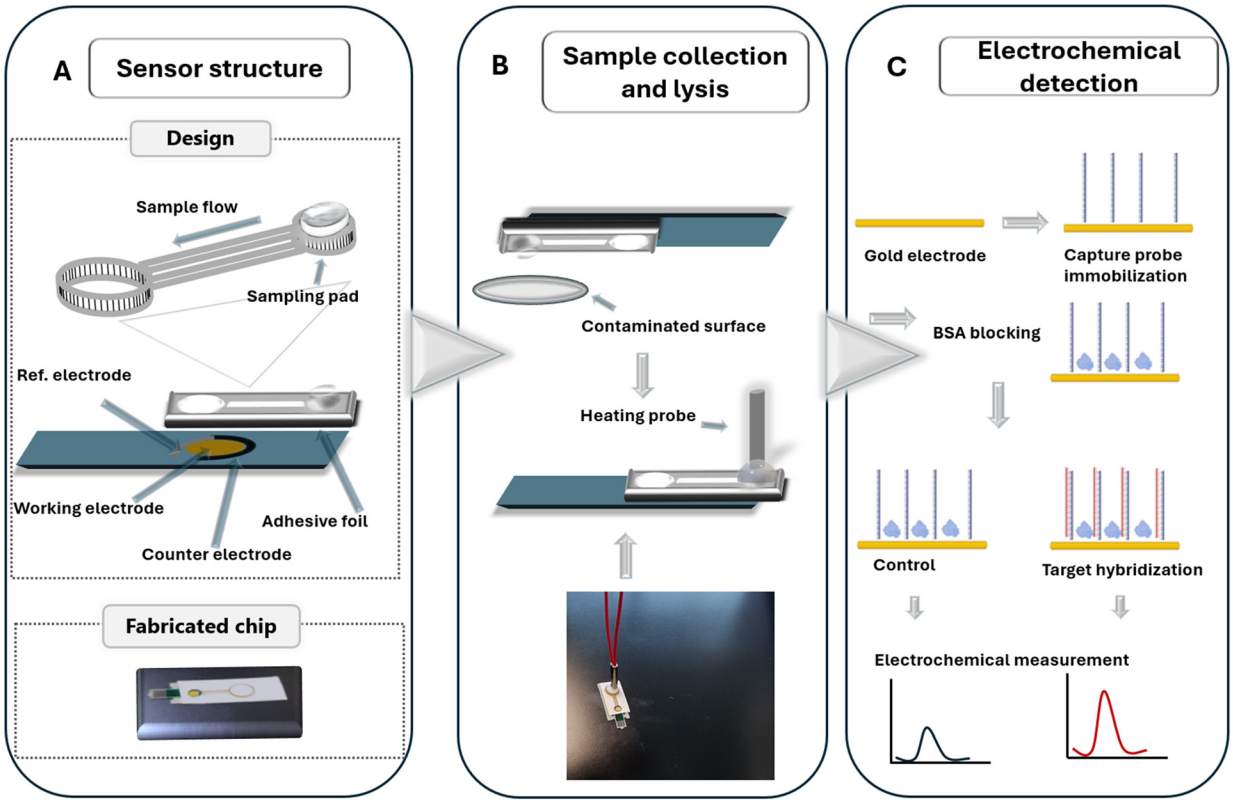

Scheme 1 Showing the layout of the integrated electrochemical sensing platform for the detection of non-coding RNA. A) The screen-printed electrode chip with the double-sided foil and fabricated chip; B) the paper pad swabbed on the contaminated surface and placed on the heating probe for thermal lysing; C) the electrode fabrication steps and detection mechanism. Non-coding RNA detection by the developed electrochemical sensor.

electrochemical measurement. The paper pad was hydrated with 50 μL of Tris-HCl buffer and swabbed over the contaminated surface. The sampling pad was then placed under a thermal probe for five minutes at 95 °C. The sample was allowed to flow to the electrode surface *via* capillary action to facilitate the hybridization of the *A. baumannii* ncRNA with the capture probe. Then the sensor was rinsed with PBS. The electrochemical measurement was performed as outlined in the preceding section.

2.5. Electrochemical detection

In this study, we developed a sensor using a three-electrode format, resulting in a device suitable for label-free testing. Briefly, each gold working electrode was functionalized by drop-casting 20 microliters of the thiolated single-strand oligonucleotide (capture probe) (SH-C6- 5′ATTACAAGTCA GTTGCTCTACCAACTGAGCTATGCCGGC-3′) prepared in 1 M Tris-HCl buffer, pH 7.5 and then allowed to incubate at 4 °C overnight. The electrodes were treated with 20 μL bovine serum albumin (BSA) for one hour after the washing phase with 1 M Tris-HCl buffer, pH 7.5. This treatment avoids the non-specific binding of non-coding RNA and minimizes background noise. At 25 °C, the incubation process is carried out for one hour. Immediately after the washing phase with 1 M Tris-HCl buffer, pH 7.5, square wave voltammetry (SWV) measurements were conducted utilizing a 10 mM solution of $[Fe(CN)_6]^{3-/4-}$. Then, the electrode was rinsed with 1 M Tris-HCl buffer. After that, the target sequence of ncRNA (5′GCCGGCATAGCTCAGTTGGTAGAGCA ACTGACTTGTAAT-3′) was incubated for one hour. The electrode was subsequently rinsed with 1 M Tris-HCl buffer, after which square wave voltammetry (SWV) measurements were conducted utilizing 10 mM $[Fe(CN)_6]^{3-/4-}$. The response variable applied to evaluate the efficacy of the procedure was the ratio of the recorded current with square wave voltammetry (SWV) before and after incubating the target sequence $((i_1-i_0)/i_0 \times 100$, where i_0 represents the baseline current and i_1 represents the target current). SWV offers high analytical performance compared to other voltammetry techniques; moreover, sensitivity is improved by reducing non-faradaic currents through differential measurement of forward and reverse pulses, allowing accurate detection of subtle changes in faradaic current associated with biomolecular interactions on the electrode surface.[33–35] The rapid voltage alternation in SWV enables fast electron transfer measurements, providing high resolution and efficient signal acquisition in a short analysis time.

3. Results and discussion

3.1. Sensor characterization

The step-by-step fabrication of an aptamer-based electrochemical sensor for non-coding RNA (ncRNA) detection is described using cyclic voltammetry (CV) in a 10 mM solution containing $[Fe(CN)_6]^{3-/4-}$ and PBS. These techniques were used to confirm the successful electrode surface modification at each stage of the sensor preparation. These methods also confirmed ncRNA hybridization model and showed sensor behavior pre- and post-hybridization.

Initially, the bare gold electrode exhibited a well-defined redox peak, indicating unimpeded electron transfer. After immobilizing the thiolated aptamer, the peak current decreased, confirming the formation of a negatively charged aptamer layer, which partially blocked electron transfer between the redox probe and the electrode surface. Subsequent blocking with BSA further reduced the peak current, as the remaining gold active sites were passivated to reduce non-specific adsorption.

Upon hybridization with the complementary ncRNA target, an increase in the redox current was observed. This change could be attributed to the surface-bound probe undergoing a conformational transition from a flexible single-stranded structure to a double-stranded helix, allowing the DNA layer to extend away from the electrode surface. This reduces steric hindrance and reduces the interface, allowing negatively charged redox ions to access the electrode surface more easily. This results in a significant increase in the SWV peak current, indicating successful hybridization of the target RNA (Fig. 1).

3.2. Optimization of the sensor

For the purpose of improving the sensor's ability to detect non-coding RNA in a sensitive and selective manner, the concentrations of the reagents utilized in each phase were optimized in the following step. During this optimization process, it was necessary to maintain a consistent concentration of the target ncRNA at 1 μM while simultaneously examining the concentrations of the capture probe and BSA. During the experiment, the concentrations were evaluated at two different levels: the capture probe was tested at concentrations of 1, 5, 10, and 20 μM, and the BSA was tested at concentrations of 0.5, 1, and 3% w/v. By carrying out a 23-full factorial design, which resulted in a total of 12 runs, it was possible to investigate the levels for each parameter. The target sequence was incubated at 60 °C, which is 20 °C below its melting temperature (T_m). This temperature was subsequently optimized.

To design the experiments (23-full factorial design), the statistical software Minitab, developed at State College, Pennsylvania, was employed. The optimal concentrations for the capture probe and BSA that yield the highest current values were established through 12 experiments, systematically assessing the ratio at each combination. This facilitated the identification of the optimal concentrations. The experiments were conducted in triplicate for every combination, both in the presence and absence of the target non-coding RNA. Table 1 summarizes the 12 experiments executed in the 23-full factorial design, including the levels of each variable.

The biggest difference between the target's current value and the baseline was produced by a combination of 20 μM of the capture probe and 0.5% w/v of BSA, as illustrated in Fig. 2. As a result, this combination was the most suitable option for *A. baumannii* non-coding RNA detection (experiment no. 10).

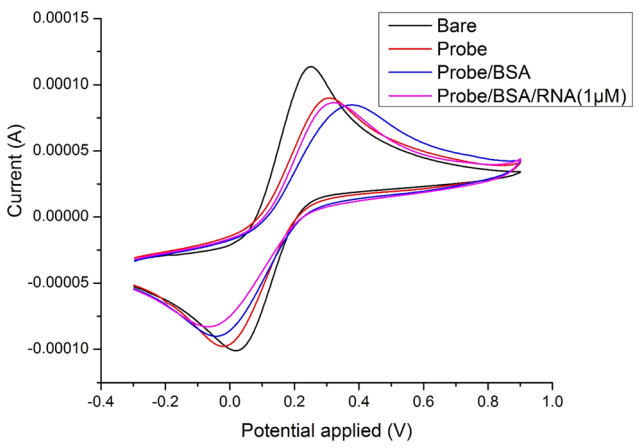

Fig. 1 Cyclic voltammetry (CV) characterization of the sensor at different fabrication stages.

3.3. Optimization of the hybridization temperature

Following the optimization of the concentrations of the capture probe and BSA, the temperature at which the hybridization was performed was next optimized: 60 °C was the initial hybridization temperature for optimizing the sensor in the previous section. This temperature was determined to be 20 degrees below the melting temperature (T_m). Using an online tool (http://biotools.nubic.northwestern.edu/OligoCalc.html), the basic T_m was determined to be 80.9 °C.

Table 1 Summary of tests conducted in the 23-factorial design

Experiment number	Capture probe (μM)	BSA (% w/v)
1	1	0.5
2	1	1
3	1	3
4	5	0.5
5	5	1
6	5	3
7	10	0.5
8	10	1
9	10	3
10	20	0.5
11	20	1
12	20	3

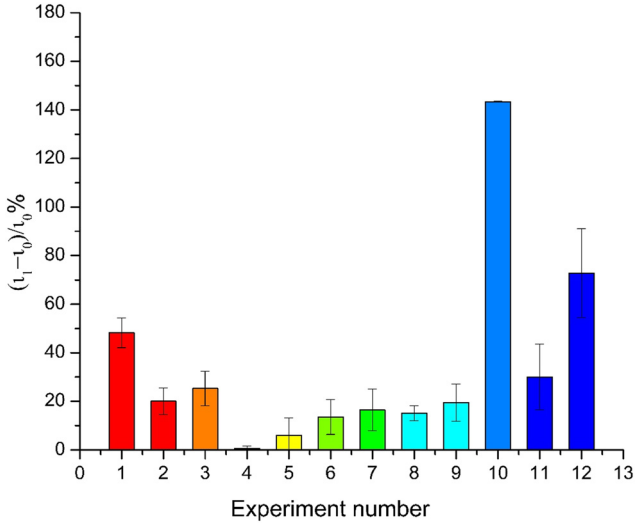

Fig. 2 Overview of measurements across various combinations(*Y*-axis values denote the ratio of each peak current to its respective control value in Tris-HCl; standard deviations of three measurements are shown by error bars).

The hybridization temperature was optimized by incubating 1 μM of the target ncRNA in a wide range of temperatures for one hour. This step was necessary to further enhance the sensor's performance and account for the significant impact of hybridization temperature on its sensitivity. Fig. 3 shows that the hybridization temperature has an impact on the sensitivity of the sensor. These findings also indicate that the optimal temperature for the incubation of this sample for electrochemical detection is 25 °C. Although hybridization was initially evaluated near the calculated T_m, we observed that a lower temperature (25 °C) yielded a stronger electrochemical signal. This effect can be attributed to the surface-confined hybridization kinetics on the electrode, which differs from that in the bulk solution. At lower temperatures, the hybrid divalent remains more stable, and the target capture rate on the surface is higher, resulting in greater hybridization efficiency and improved signal response. Furthermore, the presence of Tris-HCl buffer in the hybridization solution likely contributed to a shift in the effective T_m, resulting in the stability of the divalent at lower temperatures.[36,37]

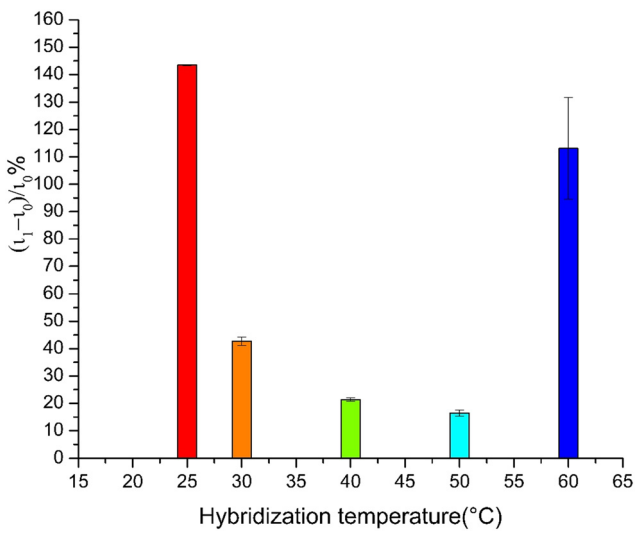

Fig. 3 Optimization of the hybridization temperature (*Y*-axis values denote the ratio of each peak current to its respective control value in Tris-HCl; standard deviations of three measurements are shown by error bars).

3.4. Sensor performance

Sensor sensitivity is a critical characteristic, as it determines the ability of the sensor to accurately detect the target substance in the sample. To assess the sensitivity of this sensor for detecting non-coding RNA, a calibration curve was

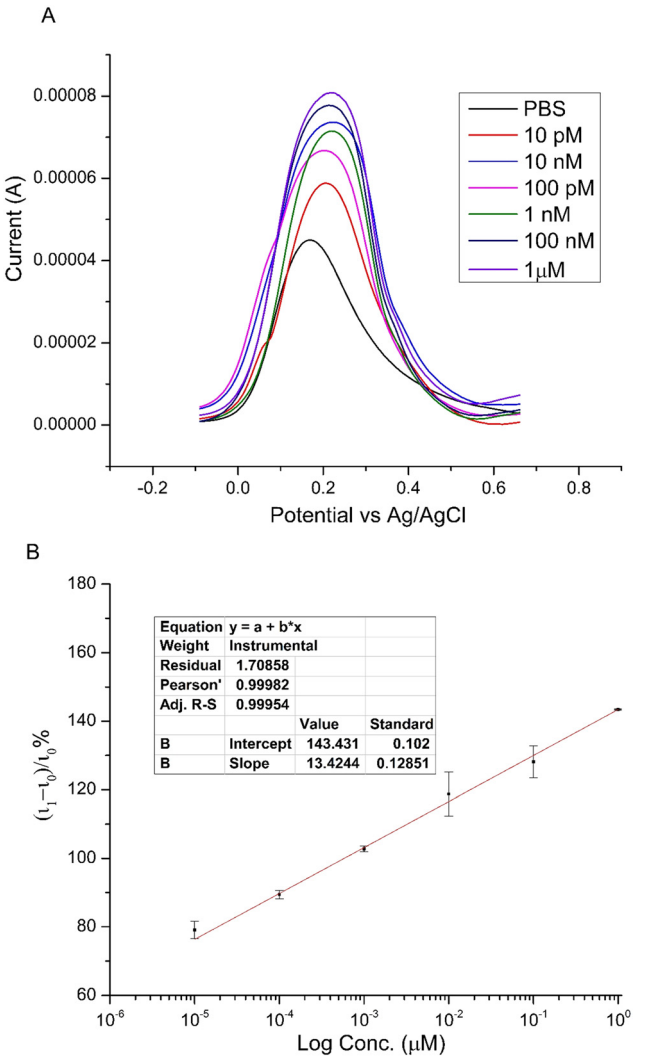

Fig. 4 A) Calibration curve correspondence voltammograms for each concentration; B) *A. baumannii* non-coding RNA calibration curves (*Y*-axis values denote the ratio of each peak current to its respective control value in Tris-HCl, standard deviations of three measurements are shown by error bars).

generated using various concentrations of non-coding RNA prepared in Tris-HCl, along with the optimized sensor and optimal hybridization temperature. Data were fitted using the curve in Fig. 4(A), where y is the ratio of the current and x is the concentration of the non-coding RNA. Fig. 4(B) illustrates the voltammograms of the concentrations represented in Fig. 4(A); these voltammograms show an increase in current with increasing concentrations of non-coding RNA. To ensure reliable and consistent sensor performance and evaluate the reproducibility of the developed non-coding RNA sensor, the calibration curve was recorded using n = 6 independent sensors to assess inter-chip reproducibility, while each measurement on a given sensor was repeated three times (n = 3) to determine intra-chip reproducibility. The resulting data were expressed as average values with standard deviations, and error bars were included in the calibration plot to reflect measurement variability.

The limit of quantitation (LoQ) and the limit of detection (LoD) are important concepts in analytical measurements. The former specifies the lowest concentration at which an analyte can be quantitatively detected with an acceptable level of precision and accuracy, while the latter indicates the lowest concentration at which a substance can be reliably distinguished from its absence (a blank sample). The formulas that follow illustrate how both parameters were determined: LoD = 3.3(Sy/S) and LoQ = 10(Sy/S), where Sy is the standard deviation of the response and S is the slope of the calibration curve. The LoD was determined to be 5 pM and the LoQ to be 15 pM.

Sensor selectivity denotes a sensor's capacity to accurately identify and distinguish specific target analytes amidst various interfering substances. This attribute is essential for guaranteeing the reliability and precision of sensor data, especially in intricate situations where various substances may coexist.

Two nonspecific ncRNA sequences from *Salmonella* (5′TGAA CCGCATCAGCACCACCACCATTACCACCATCACCATTACCAC AGGTAACGGTGCGGGCT-3′) and *Pseudomonas* (5′GTCCTCTGA TCTGCGTACATCTCCGGTAAACACTGACCTCGACGATCAGAA CCGTA-3′) were used with a 1 μM concentration to explore the selectivity of the sensor.

Alignments of both *Salmonella* and *Pseudomonas* ncRNA showed low to moderate sequence matching with the *A. baumannii* RNA, enabling the assessment of cross-hybridization potential while maintaining sufficient divergence from the target. Both sequences exhibit GC-rich domains and are anticipated to develop secondary structures similar to *A. baumannii* RNA. Consequently, these sequences were used to validate the sensor's selectivity.

While the current was nearly unchanged after incubating the control sequences from *Salmonella* and *Pseudomonas*, the current increased following incubation of the target ncRNA (*A. baumannii*), confirming that the sensor is highly selective to the target sequence (Fig. 5).

To evaluate the ability of the sensor to detect the target sequence in real samples, samples from bacterial cultures

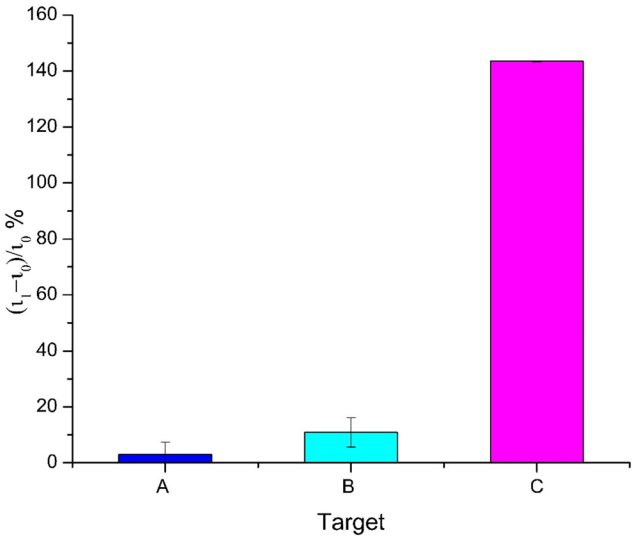

Fig. 5 Selectivity of the sensor using 1 μM nonspecific ncRNA sequences from A) *Salmonella*, B) *Pseudomonas* and C) 1 μM target ncRNA (*A. baumannii*) (*Y*-axis values denote the ratio of each peak current to its respective control value in Tris-HCl; standard deviations of three measurements are shown by error bars).

were used. Following the cultivation of *Acinetobacter baumanni* (ATCC 19606) in a nutrient broth for 24 hours at 37 °C, cells of the bacteria were lysed to extract their components for use as sensor recognition elements. The lysed cells were filtered through a 0.2 μm filter to minimize the non-specific binding of the components of the bacterial cell to the electrode surface. Following that, 20 μL of the eluted sample was placed onto the electrode and incubated for one hour using the optimal conditions. The findings shown in Fig. 6 demonstrate the sensor's capability to identify the particular sequence of genuine samples of bacteria.

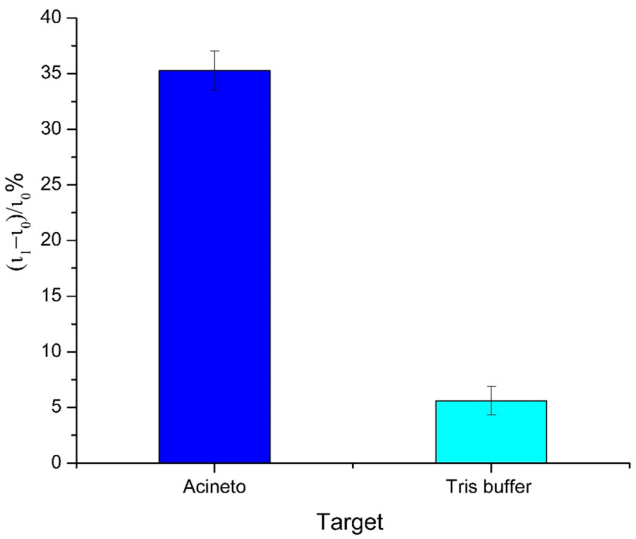

Fig. 6 Validation with bacterial from bacterial cultures samples (*Y*-axis values denote the ratio of each peak current to its respective control value in Tris-HCl; standard deviations of three measurements are shown by error bars).

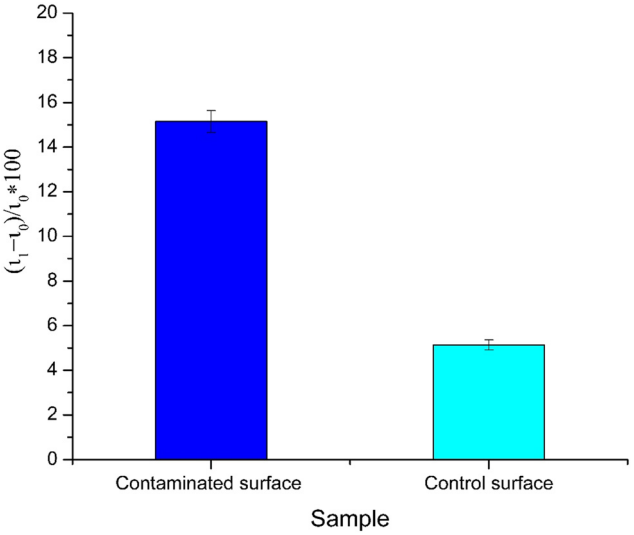

Fig. 7 The results from the *A. baumannii* contaminated surface and control surface without bacteria, followed with thermal lysis and detection (*Y*-axis values denote the ratio of each peak current to its respective control value in Tris-HCl; standard deviations of three measurements are shown by error bars).

The final design of the sensor, depicted in Scheme 1, was assessed to determine its efficacy in collecting and detecting the target bacteria from contaminated surfaces. In summary, one surface was inoculated with bacteria from cultures *via* a swab, while the other surface was steralized. The final sensor was employed to gather samples from both surfaces, followed by the application of the detection protocol as outlined in the methodology section. Fig. 7 illustrates that the current has increased in sensors employed for contaminated surfaces, whereas no variation has been observed in disinfected surfaces.

This sensor is the first of its type to be constructed for the detection of non-coding RNA (ncRNA) from genuine bacterial samples, with an integrated sample collection pad. All previous sensors developed for *A. baumannii* were either able to detect the whole bacterium by using aptamers or modifying the electrode surface,[24] or were able to detect the DNA of the bacteria,[22,38,39] which required DNA extraction before being amplified and detected, which is not necessary in this sensor.

This detection strategy can be improved, paving the way for the development of a portable device that integrates online lysis and detection, enabling bacterial detection in healthcare settings for diagnosis in remote or resource-limited areas. In this work, the developed sensor offers direct molecular detection of the bacteria by detecting specific ncRNA sequences, and a detection stream requiring only cell lysis.

Conclusion

We have developed a sensitive and selective electrochemical sensor for the collection, lysing, and detection of non-coding RNA (ncRNA) in *Acinetobacter baumannii*. The sensor relies on the hybridization of target ncRNAs with complementary thiolated sequences fixed on a gold electrode. Square-wave voltammetry (SWV) was used to precisely measure the resulting current change. The integration of sample-collecting platforms enables direct sampling from contaminated surfaces, followed by a straightforward thermal lysis procedure using a thermal probe, making the sensor user-friendly and practical. The sensor has high analytical performance, with a detection limit of 5 pM and 15 pM LoQ, and has been effectively used for the detection of ncRNAs in cell culture samples. These findings highlight the platform's capability for the fast and direct identification of bacteria without the need for equipped labs. The sensor may be developed into a comprehensive device for sample collection, cellular analysis, and bacterial detection in hospitals and healthcare settings, enabling the identification of germs without the need for intricate testing procedures.

Conflicts of interest

There are no conflicts to declare.

Data availability

The processed data that support the findings of this study are available from the corresponding author upon reasonable request.

Acknowledgements

The authors wolud like to acknowledge the generous funding from Alfaisal University.

References

1 L. L. Maragakis and T. M. Perl, Acinetobacter baumannii: Epidemiology, antimicrobial resistance, and treatment options, *Clin. Infect. Dis.*, 2008, **46**, 1254–1263, DOI: 10.1086/529198/2/46-8-1254-TBL002.GIF.
2 M. Carvalho, T. Bento de Carvalho, J. B. Barbosa, P. Teixeira and E. Bergogne-Bérézin, *Encycl. Food Safety*, 2nd edn, 2023, vol. 1–4, pp. V2-58–V2-67.
3 V. Rebic, N. Masic, S. Teskeredzic, M. Aljicevic, A. Abduzaimovic and D. Rebic, The Importance of Acinetobacter Species in the Hospital Environment, *Med. Arch.*, 2018, **72**, 325, DOI: 10.5455/MEDARH.2018.72.330-334.
4 S. Fahy, J. A. O'Connor, B. Lucey and R. D. Sleator, *Br. J. Biomed. Sci.*, 2023, **80**, 11098.
5 B. Basatian-Tashkan, M. Niakan, M. Khaledi, H. Afkhami, F. Sameni, S. Bakhti and R. Mirnejad, Antibiotic resistance assessment of Acinetobacter baumannii isolates from Tehran hospitals due to the presence of efflux pumps encoding genes (adeA and adeS genes) by molecular method, *BMC Res. Notes*, 2020, **13**, 1–6, DOI: 10.1186/S13104-020-05387-6/TABLES/3.

6 R. Vázquez-López, S. G. Solano-Gálvez, J. J. J. Vignon-Whaley, J. A. A. Vaamonde, L. A. P. Alonzo, A. R. Reséndiz, M. M. Álvarez, E. N. V. López, G. Franyuti-Kelly, D. A. Álvarez-Hernández, V. M. Guzmán, J. E. J. Bañuelos, J. M. Felix, J. A. G. Barrios and T. B. Fortes, Acinetobacter baumannii Resistance: A Real Challenge for Clinicians, *Antibiotics*, 2020, **9**, 205, DOI: 10.3390/ANTIBIOTICS9040205.

7 I. Kyriakidis, E. Vasileiou, Z. D. Pana and A. Tragiannidis, Acinetobacter baumannii Antibiotic Resistance Mechanisms, *Pathogens*, 2021, **10**, 3390, DOI: 10.3390/PATHOGENS10030373.

8 P. Espinal, S. Martí and J. Vila, Effect of biofilm formation on the survival of Acinetobacter baumannii on dry surfaces, *J. Hosp. Infect.*, 2012, **80**, 56–60, DOI: 10.1016/J.JHIN.2011.08.013.

9 A. Gedefie, W. Demsis, M. Ashagrie, Y. Kassa, M. Tesfaye, M. Tilahun, H. Bisetegn and Z. Sahle, Acinetobacter baumannii Biofilm Formation and Its Role in Disease Pathogenesis: A Review, *Infect. Drug Resist.*, 2021, **14**, 3711, DOI: 10.2147/IDR.S332051.

10 J. A. Gaddy and L. A. Actis, Regulation of Acinetobacter baumannii biofilm formation, *Future Microbiol.*, 2009, **4**, 273, DOI: 10.2217/FMB.09.5.

11 S. E. Weinberg, A. Villedieu, N. Bagdasarian, N. Karah, L. Teare and W. F. Elamin, Control and management of multidrug resistant Acinetobacter baumannii: A review of the evidence and proposal of novel approaches, *Infect. Prev. Pract.*, 2020, **2**, 100077, DOI: 10.1016/J.INFPIP.2020.100077.

12 K. Rangel and S. G. De-Simone, Treatment and Management of Acinetobacter Pneumonia: Lessons Learned from Recent World Event, *Infect. Drug Resist.*, 2024, **17**, 507–529, DOI: 10.2147/IDR.S431525.

13 Y. Jiang, Y. Ding, Y. Wei, C. Jian, J. Liu and Z. Zeng, Carbapenem-resistant Acinetobacter baumannii: A challenge in the intensive care unit, *Front. Microbiol.*, 2022, **13**, 1045206, DOI: 10.3389/FMICB.2022.1045206/BIBTEX.

14 K. A. Thom, T. Howard, S. Sembajwe, A. D. Harris, P. Strassle, B. S. Caffo, K. C. Carroll and J. K. Johnson, Comparison of Swab and Sponge Methodologies for Identification of Acinetobacter baumannii from the Hospital Environment, *J. Clin. Microbiol.*, 2012, **50**, 2140, DOI: 10.1128/JCM.00448-12.

15 X. Corbella, M. Pujol, M. J. Argerich, J. Ayats, M. Sendra, C. Peña and J. Ariza, Environmental sampling of Acinetobacter baumannii: moistened swabs versus moistened sterile gauze pads, *Infect. Control Hosp. Epidemiol.*, 1999, **20**, 458–460, DOI: 10.1086/503137.

16 I. Yusuf, H. B. Idris, E. Skiebe and G. Wilharm, Local Genomic Epidemiology of Acinetobacter baumannii Circulating in Hospital and Non-hospital Environments in Kano, Northwest Nigeria, *Curr. Microbiol.*, 2025, **82**, 329, DOI: 10.1007/S00284-025-04304-Z.

17 K. Abdelkader, D. Gutiérrez, D. Grimon, P. Ruas-Madiedo, C. Lood, R. Lavigne, A. Safaan, A. S. Khairalla, Y. Gaber, T. Dishisha and Y. Briers, Lysin LysMK34 of Acinetobacter baumannii Bacteriophage PMK34 Has a Turgor Pressure-Dependent Intrinsic Antibacterial Activity and Reverts Colistin Resistance, *Appl. Environ. Microbiol.*, 2020, **86**, DOI: 10.1128/AEM.01311-20.

18 N. Pal, P. Sharma, S. Singh, M. Kumawat, S. K. Snehi, A. Tilwari, R. R. Tiwari, D. K. Sarma and M. Kumar, Isolation and characterization of lytic bacteriophages against multi drug-resistant Acinetobacter baumannii, *Microb. Pathog.*, 2025, **208**, 107982, DOI: 10.1016/J.MICPATH.2025.107982.

19 H. T. Gozdas, Diagnosis of Acinetobacter Baumannii Infections, *Int. J. Prev. Med.*, 2012, **3**, 817.

20 A. I. Bagudo, G. A. Obande, A. Harun and K. K. B. Singh, Advances in automated techniques to identify Acinetobacter calcoaceticus–Acinetobacter baumannii complex, *Asian Biomed.*, 2020, **14**, 177, DOI: 10.1515/ABM-2020-0026.

21 M. A. F. Khalil, H. M. E. Azzazy, A. S. Attia and A. G. M. Hashem, A sensitive colorimetric assay for identification of Acinetobacter baumannii using unmodified gold nanoparticles, *J. Appl. Microbiol.*, 2014, **117**, 465–471, DOI: 10.1111/JAM.12546.

22 F. Bahavarnia, P. Pashazadeh-Panahi, M. Hasanzadeh and N. Razmi, DNA based biosensing of Acinetobacter baumannii using nanoparticles aggregation method, *Heliyon*, 2020, **6**, e04474, DOI: 10.1016/J.HELIYON.2020.E04474.

23 S. Kanapathy, G. A. Obande, C. Chuah, R. H. Shueb, C. Y. Yean and K. K. Banga Singh, Sequence-Specific Electrochemical Genosensor for Rapid Detection of blaOXA-51-like Gene in Acinetobacter baumannii, *Microorganisms*, 2024, 2076, DOI: 10.3390/MICROORGANISMS10071413.

24 M. Roushani, M. Sarabaegi and A. Rostamzad, Novel electrochemical sensor based on polydopamine molecularly imprinted polymer for sensitive and selective detection of Acinetobacter baumannii, *J. Iran. Chem. Soc.*, 2020, **17**, 2407–2413, DOI: 10.1007/S13738-020-01936-9.

25 C. Singhal, S. Gupta, J. Dhingra, S. Pandey, S. Chatterjee, R. Bargakshatriya, D. K. Avasthi, S. Pramanik and S. Chaudhuri, Label-free electrochemical aptasensor for detection of Acinetobacter baumannii: Unveiling the kinetic behavior of reduced graphene oxide v/s graphene oxide, *Electrochim. Acta*, 2024, **492**, 144240, DOI: 10.1016/J.ELECTACTA.2024.144240.

26 F. Hubé and C. Francastel, Coding and Non-coding RNAs, the Frontier Has Never Been So Blurred, *Front. Genet.*, 2018, **9**, 140, DOI: 10.3389/FGENE.2018.00140.

27 P. Zhang, W. Wu, Q. Chen and M. Chen, Non-Coding RNAs and their Integrated Networks, *J. Integr. Bioinform*, 2024, DOI: 10.1515/JIB-2019-0027.

28 S. Bhowmik, A. Pathak, S. Pandey, K. Devnath, A. Sett, N. Jyoti, T. Bhando, J. Akhter, S. Chugh, R. Singh, T. K. Sharma and R. Pathania, Acinetobacter baumannii represses type VI secretion system through a manganese-dependent small RNA- mediated regulation, *MBio*, 2024, **16**, e03025-24, DOI: 10.1128/MBIO.03025-24.

29 F. J. Hamrock, D. Ryan, A. Shaibah, A. S. Ershova, A. Mogre, M. M. Sulimani, S. Ben Taarit, S. Reichardt, K. Hokamp, A. J. Westermann and C. Kröger, Global analysis of the RNA–RNA interactome in Acinetobacter baumannii AB5075 uncovers a

small regulatory RNA repressing the virulence-related outer membrane protein CarO, *Nucleic Acids Res.*, 2024, **52**, 11283–11300, DOI: 10.1093/NAR/GKAE668.

30 M. Sarshar, D. Scribano, A. T. Palamara, C. Ambrosi and A. Masotti, The Acinetobacter baumannii model can explain the role of small non-coding RNAs as potential mediators of host-pathogen interactions, *Front. Mol. Biosci.*, 2022, **9**, 1088783, DOI: 10.3389/FMOLB.2022.1088783.

31 J. L. Allen, B. R. Tomlinson, L. G. Casella and L. N. Shaw, Regulatory Networks Important for Survival of Acinetobacter baumannii within the Host, *Curr. Opin. Microbiol.*, 2020, **55**, 74, DOI: 10.1016/J.MIB.2020.03.001.

32 T. R. Cech and J. A. Steitz, The Noncoding RNA Revolution—Trashing Old Rules to Forge New Ones Thomas, *Cell*, 2014, **157**, 77–94, DOI: 10.1016/J.CELL.2014.03.008.

33 V. Mirceski, D. Guziejewski, L. Stojanov and R. Gulaboski, Differential Square-Wave Voltammetry, *Anal. Chem.*, 2019, **91**, 14904–14910, DOI: 10.1021/ACS.ANALCHEM.9B03035.

34 M. D. Holtan, S. Somasundaram, N. Khuda and C. J. Easley, Non-Faradaic Current Suppression in DNA Based Electrochemical Assays with a Differential Potentiostat, *Anal. Chem.*, 2019, **91**, 15833, DOI: 10.1021/ACS.ANALCHEM.9B04149.

35 S. W. Abeykoon and R. J. White, Continuous Square Wave Voltammetry for High Information Content Interrogation of Conformation Switching Sensors, *ACS Meas. Sci. Au*, 2022, **3**, 1–9, DOI: 10.1021/ACSMEASURESCIAU.2C00044.

36 W. Qiao, H. C. Chiang, H. Xie and R. Levicky, Surface vs Solution Hybridization: Effects of Salt, Temperature, and Probe Type, *Chem. Commun.*, 2015, **51**, 17245, DOI: 10.1039/C5CC06674C.

37 Y. Gao, L. K. Wolf and R. M. Georgiadis, Secondary structure effects on DNA hybridization kinetics: a solution versus surface comparison, *Nucleic Acids Res.*, 2006, **34**, 3370–3377, DOI: 10.1093/NAR/GKL422.

38 L. Statello, C. J. Guo, L. L. Chen and M. Huarte, Gene regulation by long non-coding RNAs and its biological functions, *Nat. Rev. Mol. Cell Biol.*, 2020, **22**, 96–118, DOI: 10.1038/s41580-020-00315-9.

39 P. Li, W. Niu, H. Li, H. Lei, W. Liu, X. Zhao, L. Guo, D. Zou, X. Yuan, H. Liu, J. Yuan and C. Bai, Rapid detection of Acinetobacter baumannii and molecular epidemiology of carbapenem-resistant A. baumannii in two comprehensive hospitals of Beijing, China, *Front. Microbiol.*, 2015, **6**, DOI: 10.3389/FMICB.2015.00997.